5352 *J. Am. Chem. Soc.* **2001,** *123,* 5352−5353

α-Iminocarboxamidato−Nickel(II) Ethylene Polymerization Catalysts

Bun Yeoul Lee, Guillermo C. Bazan,* Javier Vela,
Zachary J. A. Komon, and Xianhui Bu

Departments of Chemistry and Materials
University of California, Santa Barbara, California 93106

Received December 7, 2000

Nickel-based olefin polymerization and oligomerization catalysts have attracted considerable recent attention.[1,2] Depending on the ancillary ligand framework, these catalysts participate in chain-walking reactions,[3,4] tolerate polar functionalities on the monomer,[5] and may even be used in water.[6] These properties allow for the synthesis of materials with unique topologies[7] and could enable new industrial processes.[2]

During our efforts at developing tandem catalytic processes,[8] we discovered that the reactivity of SHOP-type catalysts such as $[(C_6H_5)_2PC_6H_4C(O)O\text{-}\kappa^2P,O]Ni(\eta^3\text{-}CH_2CMeCH_2)$[9] increases considerably upon addition of $B(C_6F_5)_3$. Carbonyl coordination to the borane gives $[(C_6H_5)_2PC_6H_4C(O{-}B(C_6F_5)_3)O\text{-}\kappa^2P,O]Ni(\eta^3\text{-}CH_2CMeCH_2)$ and removes electron density from nickel. This "activation" by action of a Lewis acid on a site removed from the monomer insertion trajectory prompted our attention. The more common situation reduces to methyl abstraction and coordination of the resulting borate anion.[10] Borate dissociation from the metal is a generally accepted requirement for olefin insertion.[11]

It occurred to us that metal activation by formation of carbonyl adducts could form the basis of a new strategy for designing novel nickel olefin polymerization catalysts such as **1**−**3**. Resonance structures **I** and **II** illustrate the loss of electron density at nickel.

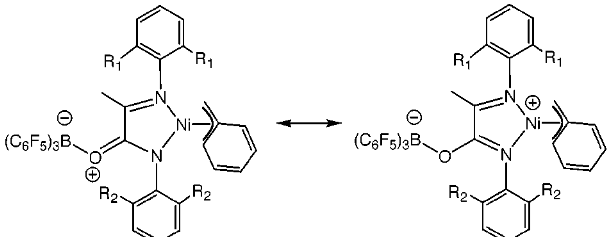

I

1, $R_1 = R_2 = H$
2, $R_1 = CHMe_2$, $R_2 = H$
3, $R_1 = R_2 = CHMe_2$

II

Scheme 1[a]

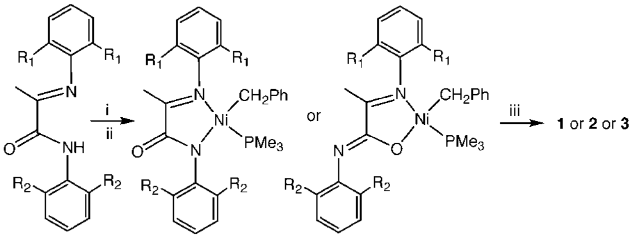

4, $R_1 = R_2 = H$
5, $R_1 = CHMe_2$, $R_2 = H$

6, $R_1 = R_2 = CHMe_2$

[a] i) KH; ii) $Ni(\eta^3\text{-}CH_2C_6H_5)Cl(PMe_3)$; iii) 2 $B(C_6F_5)_3$.

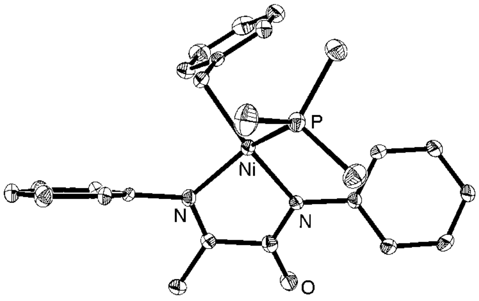

Figure 1. ORTEP drawing of **4** drawn at 30% probability. Hydrogen atoms not shown for clarity.

α-Iminocarboxamide ligands were chosen because they can be readily prepared and because the size of the substituents on nitrogen can be varied to modulate steric effects. Of interest to us was to control the size of the substituents on the pseudoaxial sites, since blocking these sites in other nickel catalysts reduces chain transfer to the monomer.[1,12] The η^3-benzyl fragment was selected, instead of the more frequently used methallyl, because it displays faster rates of initiation.[13]

Typical Schiff-base condensation[14] of primary arylamines with *N*-aryl pyruvamides[15] yields α-iminocarboxamides. As shown in Scheme 1, carboxamide deprotonation with 1.0 equiv KH, followed by reaction with $Ni(\eta^3\text{-}CH_2C_6H_5)Cl(PMe_3)$,[16] results in the clean formation of the α-iminocarboxamide complexes **4** ($R_1 = R_2 = H$), **5** ($R_1 = CHMe_2$, $R_2 = H$), and **6** ($R_1 = R_2 = CHMe_2$). Recrystallization from benzene by slow diffusion of pentane vapor at room temperature (**4** and **5**), or pentane at −30 °C (**6**), affords analytically pure **4**−**6** in 70−80% yields.

Structural characterization of **4** (Figure 1) reveals a distorted square-planar geometry (interplane angle of NNiN and CNiP planes: 42.2°) with a trans relationship between PMe_3 and the imine nitrogen. The distance between Ni and the carboxamide-N is shorter (1.936(2) Å) than that between Ni and the imine-N (2.001(3) Å); the C−O distance (1.243 (4) Å) is consistent with a double bond between these two atoms. In **6**, it is the carboxamide oxygen that coordinates to nickel (Figure 2), and the ligand environment is strictly square-planar (interplane angle of NNiO and CNiP planes: 4.3°). The C−O distance in **6** is longer (1.302(3) Å) than that of **4**, consistent with a reduced π interaction.

Single crystals of **5** suitable for X-ray diffraction studies are not available at this stage. However, the ^{31}P NMR chemical shifts in C_6D_6 are sensitive to the carboxamide binding mode. In **4** (N-bound), one observes a signal at −24.6 ppm, while for **6** (O-bound) the signal appears at −10.0 ppm. For **5**, the PMe_3

---

(1) Johnson, L. K.; Killian, C. M.; Brookhart, M. *J. Am. Chem. Soc.* **1995**, *117*, 6414.

(2) Reviews: (a) Ittel, S. D.; Johnson, L. K.; Brookhart, M. *Chem. Rev.* **2000**, *100*, 1169. (b) Mecking, S. *Coord. Chem. Rev.* **2000**, *203*, 325.

(3) Möhring, V. M.; Fink, G. *Angew. Chem., Int. Ed. Engl.* **1985**, *24*, 1001.

(4) Guan, Z.; Cotts, P. M.; McCord, E. F.; McLain, S. J. *Science* **1999**, *283*, 2059.

(5) (a) Younkin, T. R.; Connor, E. F.; Henderson, J. I.; Friedrich, S. K.; Grubbs, R. H.; Banselben, D. A. *Science* **2000**, *287*, 460.

(6) (a) Held, A.; Bauers, F. M.; Mecking, S. *Chem. Commun.* **2000**, 301. (b) Bauers, F. M.; Stefan Mecking, S. *Macromolecules* **2001**, *34*, 1165.

(7) Cotts, P. M.; Guan, Z.; McCord, E.; McLain, S. *Macromolecules* **2000**, *33*, 6945.

(8) (a) Komon, Z. J. A.; Bu, X.; Bazan, G. C. *J. Am. Chem. Soc.* **2000**, *122*, 1830. (b) Barnhart, R. W.; Bazan, G. C.; Mourney, T. *J. Am. Chem. Soc.* **1998**, *120*, 1082.

(9) Bonnet, M. C.; Dahan, F.; Ecke, A.; Keim, W.; Schultz, R. P.; Tkatchenko, I. *Chem. Commun.* **1994**, 615.

(10) Chen, E. Y.-X.; Marks, T. J. *Chem. Rev.* **2000**, *100*, 1391.

(11) Substantial debate continues on this mechanistic point. For relevant discussion, see: Beck, S.; Lieber, S.; Schaper, F.; Geyer, A.; Brintzinger, H.-H. *J. Am. Chem. Soc.* **2001**, *123*, 1483.

(12) (a) Johnson, L. K.; Mecking, S.; Brookhart, M. *J. Am. Chem. Soc.* **1996**, *118*, 11664. (b) Deng, L.; Woo, T. K.; Cavallo, L.; Margl, P. M.; Ziegler, *J. Am. Chem. Soc.* **1997**, *119*, 6177. (c) Svejda, S. A.; Johnson, L. K.; Brookhart, *J. Am. Chem. Soc.* **1999**, *121*, 10634.

(13) Komon, Z. J. A.; Bu, X.; Bazan, G. C. *J. Am. Chem. Soc.* **2000**, *122*, 12379.

(14) Britovsek, G. J. P.; Bruce, M.; Gibson, V. C.; Kimberley, B. S.; Maddox, P. J.; Mastroianni, S.; McTavish, S. J.; Redshaw, C.; Solan, G. A.; Strömberg, S.; White, A. J. P.; Williams, D. J. *J. Am. Chem. Soc.* **1999**, *121*, 8728.

(15) Wang, C.-Z.; Mallat, T.; Baiker, A. *Tetrahedron: Asymmetry* **1997**, *8*, 2133.

(16) Carmona, E.; Paneque, M.; Poveda, M. L. *Polyhedron* **1989**, *8*, 285.

10.1021/ja004191h CCC: $20.00

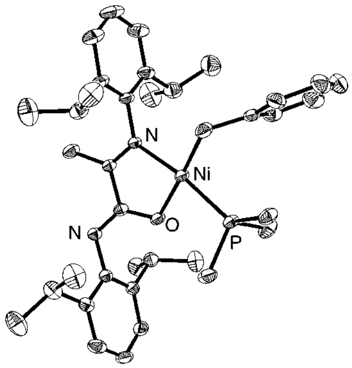

Figure 2. ORTEP drawing of **6** drawn at 30% probability. Hydrogen atoms not shown for clarity.

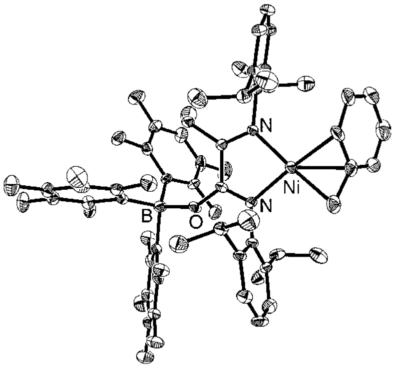

Figure 3. ORTEP drawing of **3** drawn at 30% probability. Hydrogen atoms not shown for clarity.

resonance occurs at −22.2 ppm, which strongly suggests an N-bound carboxamide, as shown in Scheme 1.

Addition of 2 equiv of $B(C_6F_5)_3$ to solutions of **4**−**6** in benzene results in the immediate precipitation of $Me_3P{-}B(C_6F_5)_3$ and the formation of **1**−**3**. ^1H NMR spectra of the products show the formation of two isomers, the ratio of which depends on the ligand environment (1:1, 3:1, 2:1 for **1**, **2**, and **3**, respectively). The upfield shift of the aromatic protons on the benzyl ligand from 7 to 8 to 5.6 to 7 ppm indicates η^3-coordination.[16] In addition, the ^{11}B NMR signal from $B(C_6F_5)_3$ changes from 59 to 0.7 ppm, consistent with the formation of a B−O adduct. Our current thinking is that the sets of isomers arise from pseudorotamers of the benzyl ligand, as shown by **A** and **B** below.

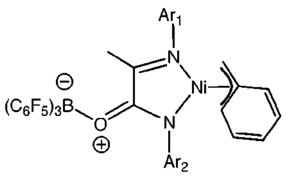

A

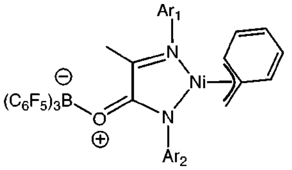

B

Examination of **6** raises the possibility of borane coordination to the carboxamide nitrogen, rather than oxygen. To resolve this uncertainty, single crystals of one isomer of **3** suitable for X-ray diffraction studies were obtained by slowly allowing layered hexane solutions of **6** and $B(C_6F_5)_3$ to diffuse at room temperature. As shown in Figure 3, compound **3** is the oxygen adduct. The two aryl rings are perpendicular to the nickel square plane and are "pushed" slightly toward nickel by the bulky fluorinated rings. Relative to the N-bound carboxamide in **4**, there is an elongation of the C−O distance (1.243(4) in **4** versus 1.288(6) Å in **3**) and a contraction of the C−N distance (1.399(4) in **4** versus 1.288(6) Å in **3**). There are nearly identical bond distances between the Ni and the two N atoms (d(Ni−N(carboxamide)) = 1.909(4) Å, d(Ni−N(imine)) = 1.942(4) Å). A substantial contribution from resonance structure **II** is therefore required to account for these structural trends.

Table 1. Reactivity toward Ethylene[a]

entry	compound	[Ni][b]	activity[c]	M_w	M_w/M_n	branches[d]	T_m
1	**4**	0.33	0				
2	**1**	0.33	1500	oligomers			
3	**2**	0.33	550	119000	25	33	125
4	**3**	0.33	350	508000	9	71	124
5	**3** + 2.5 $B(C_6F_5)_3$	0.33	510	533000	6	71	123
6	**3** + 2.5 $B(C_6F_5)_3$	0.10	850	349000	2.3	104	122
7	**3** + 2.5 $B(C_6F_5)_3$	0.10	430[e]	299000	2.8	106	122

[a] Polymerization conditions: 30 mL of toluene, 100 psig ethylene, 10 min. [b] Concentration in mM. [c] kg product/(mol Ni•h). [d] Determined by ^1H NMR, and corresponds to the number of branches/1000 carbons.[19] [e] Reaction carried out with 50 psig ethylene.

A series of ethylene polymerization studies is summarized in Table 1. No reaction is observed by using **4** (entry 1). Similar results are obtained with **5** and **6**. In the case of **1**, ethylene is consumed, quickly giving oligomers, as determined by GC/MS (entry 2). The product is a mixture of 1-alkenes, internal olefins, and 1-alkene dimers. The fraction corresponding to 1-alkenes is described by a Schultz−Flory distribution.[17] Use of **2** and **3** leads to polymer formation (entries 3 and 4). The polymer obtained with **3** is of higher molecular weight and is described by a narrower molecular-weight distribution (PDI). Comparison of entries 4 and 5 shows that adding 2.5 equiv of $B(C_6F_5)_3$ increases the activity and decreases the PDI. Lower nickel concentration gives rise to a further PDI narrowing (entries 5 and 6).[18] Reducing the pressure (entries 6 and 7) results in a drop in activity. Highest activities are obtained for **1**, probably because there is no entrapment of the catalyst within the polymer precipitate.

Analysis by ^1H NMR spectroscopy[19] shows a branched polymer structure.[1] Branching is encouraged by the bulkier ligand environment of **3**, relative to **2** (Table 1, entries 3 vs 4). Examination by ^{13}C NMR spectroscopy using established pulse sequences[20] shows a distribution of branching sizes similar to other nickel catalysts.[4] For the polymer in entry 5 one observes a majority of methyl branches (~60%), a minor component of ethyl branches (~10%) and the remainder approximately equal quantities of propyl, butyl, amyl, and long-chain branches. Lower melting points are observed with increased branching.

In summary, the synthesis and characterization of compounds **1**−**3** show that borane attachment to a site removed from the ethylene insertion trajectory can be used to activate nickel catalysts for olefin polymerization. It is interesting to note the similarities in structure/reactivity relationships to Brookhart's diimine catalysts.[1] In particular, hindering axial sites leads to substantially higher molecular weight product and the production of a branched polymer structure. The extent to which mechanistic similarities exist between compounds **2** and **3** and other nickel catalysts and how a more open reaction site leads to advantages/disadvantages for polymer synthesis are the subjects of ongoing studies.

Acknowledgment. We are grateful to the Department of Energy for financial assistance. B.Y.L. is thankful to Korea Science and Engineering Foundation for partial financial support.

Supporting Information Available: Complete details for the synthesis of all compounds, polymerization procedures, and the crystallographic studies of **3**, **4**, and **6** (PDF). This material is available free of charge via the Internet at http://pubs.acs.org.

JA004191H

---

(17) (a) Flory, P. J. *J. Am. Chem. Soc.* **1940**, *62*, 1561. (b) Schulz, G. V. *Z. Phys. Chem., Abt. B* **1935**, *30*, 379. (c) Schulz, G. V. *Z. Phys. Chem., Abt. B* **1939**, *43*, 25.

(18) Narrower PDI values are the result of better temperature control under more dilute conditions.

(19) Gates, D. P.; Svejda, S. A.; Onate, E.; Killian, C. M.; Johnson, L. K.; White, P. S.; Brookhart, M. *Macromolecules* **2000**, *33*, 2320.

(20) Galland, G. B.; de Sousa, R. F.; Mauler, R. S.; Nunes, F. F. *Macromolecules* **1999**, *32*, 1620.